

THERMAL CONDUCTIVITY INSTRUMENT FOR MEASURING PLANETARY ATMOSPHERIC PROPERTIES AND DATA ANALYSIS TECHNIQUE

B. Hathi¹*, P. M. Daniell², M. Banaszkiewicz³, A. Hagermann¹, M. R. Leese¹ and J. C. Zarnecki¹

¹Planetary and Space Sciences Research Institute, Open University, Milton Keynes, MK7 6AA, UK

²Phyworks Ltd., Bristol, BS34 8HP, UK

³Polish Academy of Sciences, Ul. Bartycka 18 A, Warsaw 00716, Poland

This paper outlines the method of measurement and analysis of the thermal conductivity instrument (THP) that has successfully returned measurements from the atmosphere of Saturn's moon Titan during the descent of the Huygens probe on 14th January 2005.

The technique is validated by analysing laboratory calibration data gathered by our instrument in three pure gases (nitrogen, methane, and ethane) over Titan's temperature range (90 to 180 K). Calibration results show errors <1% compared to reference values when processed using this method.

Details included here along with references should serve as a useful guide for interpreting data from thermal conductivity instruments for space or other stand alone applications for fluids over various pressure and temperature ranges. Our calibration only verifies measurements over Titan conditions, although [4] suggests that the validity of this method extends up to 400 atmospheres and 800°C.

Keywords: fluid, Huygens, sensor, SSP, THP, Titan

Introduction

Amongst several instruments on board the Huygens^{*} mission was a thermal conductivity instrument (THP) whose aim was to determine the thermal conductivity of the atmosphere during the descent (and of any liquid in the case of the Huygens probe landing in a hydrocarbon lake).

THP works on the hot wire principle, where heat is applied to a medium by a very thin wire and the change of wire temperature is monitored over a preset time interval. It is possible to calculate thermal conductivity of the surrounding medium from the rate of change of the wire temperature.

There are several references [1–3] which describe the design and operation of this THP.

Well documented and proven techniques exist for calculating thermal conductivity for carefully designed laboratory instruments based on the hot wire method [4, 5, 10]. To a first order, the THP instrument is also amenable to the calculation technique described in [4], but there is a need to introduce specific corrections to reduce errors in this case.

THP – design and operation

THP instrument for titan measurements consisted of four cells with each cell capable of measuring thermal

conductivity independently. Two cells were optimised for gas measurements and the other two cells were designed for measuring liquid.

Each cell consists of a 5 cm long hollow cylinder with a very thin platinum wire (5 µm radius for gas cells and 12.5 µm radius for liquid cells) suspended along the central axis. The airflow into the cylinders is restricted sufficiently to allow a measurement of the same medium to be completed during the descent phase. Each end of the thin wire is fused (i.e. welded) to two sets of platinum harnesses to allow measurement by a four wire method to minimise other external resistance.

The initial temperature is measured by applying a low current pulse of 310 µA and is immediately followed by a constant large step current of 10.355 mA. During the high current period, changes in wire resistance are recorded by spacing sampling intervals on a log_e (ln) time base.

There are several references [1–3] which describe the design and operation of this THP in more detail.

Theory of hot wire method

The change in temperature ΔT over time t of a line source at radial distance r with continuous heat supply per unit length $Q(t)$ has been given by [6] as

* Huygens probe was part of the joint NASA/ESA/ISA Cassini–Huygens mission to study Saturn and its largest moon Titan [3].

** Author for correspondence: B.Hathi@open.ac.uk

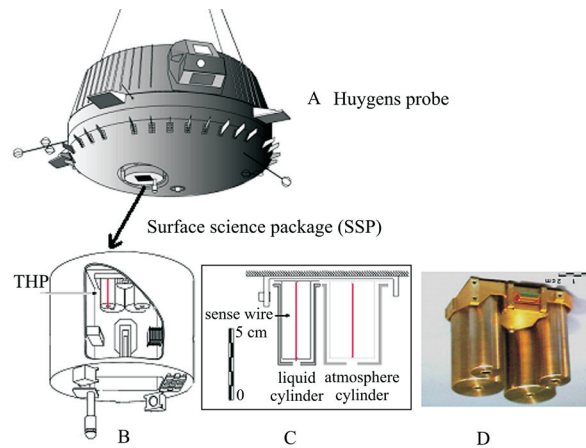


Fig. 1 A – Huygens probe in descent configuration showing the atmosphere inlet via the B – SSP’s instrument suite. THP sensor is shown in detail, C – schematic illustrating the active sensing element – a centrally suspended platinum wire, and D – photograph showing the external cylinders enclosing each wire and limiting the fluid flow within each cell

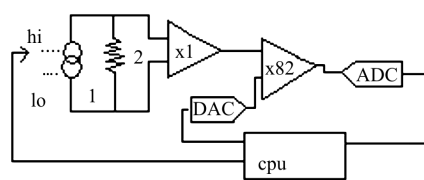


Fig. 2 Schematic of the circuit for operating the THP sensor. Each measurement begins with the cpu switching on the low constant current supply, the resulting voltage across THP wire (2) is amplified, stored, and fed back via the DAC to comparator/amplifier (x82 gain). This low current measurement gives initial resistance (R_0), from which the ambient temperature (T_0) inside the cell is obtained. T_0 is subtracted from all subsequent high current measurements. The cpu switches the high current supply (immediately after the initial measurement) and changes in wire resistance (ΔR) w.r.t. R_0 are recorded at sampling intervals spaced on ln timescale

$$\Delta T(r,t) = \int_0^t \frac{Q(t)}{4\pi\lambda} \frac{1}{t} e^{-(r^2/4\kappa t)} dt \quad (1)$$

where $\kappa = \lambda/(\rho c_p)$ is the thermal diffusivity of the surrounding medium, with thermal conductivity λ , density ρ and specific heat capacity c_p . If $Q(t)=q$ is constant, we obtain the familiar solution

$$\Delta T(r,t) = \frac{q}{4\pi\lambda} \int_{r^2/4\kappa t}^{\infty} \frac{e^{-u}}{u} du \approx \frac{q}{4\pi\lambda} [\ln(4\kappa t/r^2) - \gamma] \quad (2)$$

where $\gamma=0.5772\dots$ is Euler’s constant.

Equation (2) forms the basis of measuring thermal conductivity λ with hot wire instruments, where a thin wire is used to approximate a line source. In reality, the line source has a non-zero radius a , but it can be shown that solution (2) remains valid for large times t [6–8].

Our hot wire has a finite length l and electric resistance R , and heat is supplied by a constant current source I , therefore $q=I^2R/l$. Substituting q and rearranging (2) gives the wire temperature

$$\Delta T(t) = \frac{I^2 R}{4\pi l \lambda} \ln t + \frac{I^2 R}{4\pi l \lambda} \ln(4\kappa/a^2 e^\gamma) \quad (3)$$

where λ is found by plotting ΔT as a function of $\ln t$ and then applying a least squares fit to a region of linear increase. Selecting the correct portion of the curve is very important for the calculation of λ and will be discussed later.

THP – specific correction

The theory underlying the hot wire method assumes a constant heat flux $q=I^2R/l$ during the measurement period. However, the electrical resistance R is not constant, but can be approximated by a linear function of temperature T (and thereby $\ln t$). Hence we introduce the expression

$$q(t) = \frac{I^2}{l} R_0 + \frac{I^2}{l} \frac{d\Delta R}{d\ln t} \ln t \quad (4)$$

where R_0 =initial resistance.

Strictly speaking, q is therefore no longer a constant. Nevertheless, since $dR=d\Delta R/d\ln t \ll R_0$, Eq. (4) can still be used as a reasonable approximation. This is confirmed by our empirical tests. For a more rigorous treatment [9].

After substitution, Eq. (3) now becomes

$$\Delta T = \left[\frac{I^2 (R_0 + \ln t dR)}{4\pi l \lambda} \right] \ln t + \left[\frac{I^2 (R_0 + \ln t dR)}{4\pi l \lambda} \right] \ln(4\kappa/a^2 e^\gamma) \quad (5)$$

Differentiating (5) w.r.t. $\ln t$ results in an equation that can be used to calculate λ and will be applied later in this paper to demonstrate the method.

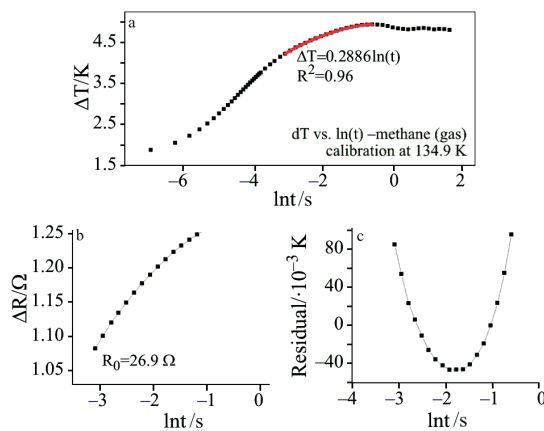


Fig. 3 a – Experimentally obtained data sampled on a logarithmic time scale from 1 ms to 5 s. The slope resulting from the lined region (after taking least squares fit of the lined region) is taken for the calculation of λ . Initial linear part of the curve cannot be used for the calculation of λ as the errors in ΔT from the finite specific heat capacity of platinum dominate the early measurements (up to the first 10 to 15 ms). Convection sets in at the top end, where the ‘transient’ regime gives way to ‘steady state’. b – Change in resistance (ΔR) vs. $\ln t$ over the region of λ calculation – used for obtaining parameters in Eq. (6). The values in this particular case (and generally) justify the assumption $d\Delta R/d\ln t \ll R_0$. c – Residuals over the region of λ calculation are calculated by subtracting the measured value of ΔT from that calculated by the least squares fit. Residuals show the presence of small but systematic errors in the first approximation of λ . Error on ΔT slope of $\pm 0.9\%$ covers most points on the ‘U’ shaped residuals plot (error calculated from residuals/ $\Delta T \sim 40$ mK/4.4 K = $\pm 0.9\%$)

$$\frac{d\Delta T}{d\ln t} = \frac{1}{4\pi\lambda} [I^2 R_0 + 2I^2 dR \ln t + I^2 dR \ln(4\kappa/a^2 e^\gamma)] \quad (6)$$

All terms except κ in Eq. (6) are known constants after a measurement run (i.e. ΔT vs. t) to calculate λ . The effect of correction (6) on λ is particularly noticeable at lower temperatures (i.e. titan conditions), where wire resistance R_0 is low and the two dR dependent terms of Eq. (6) begin to contribute to the average heat flux (or power).

Figure 3 shows the region used for calculating the first approximation value of λ .

Other corrections

Two other corrections are necessary to interpret measurements from THP. The first correction accounts for the finite specific heat capacity of platinum wire and the second deals with the walls of the hollow cylinder enclosing the hot wire.

Mathematical treatments for both corrections can be found in [4]; for our purposes it is sufficient to quote the results.

The specific heat capacity correction, as given by Eq. (7), adds a term δT_1 to the observed ΔT to account for some heat loss before a rise in wire temperature occurs. As sample time t tends to 0, the correction δT_1 tends to infinity, hence Eq. (7) only yields a useful correction after the first few milliseconds. In Eq. (7), the subscripts ‘w’ and ‘m’ denote wire and medium parameters, respectively.

$$\delta T_1 = +a^2 \frac{(\rho c_p)_w - (\rho c_p)_m}{2\lambda t} \Delta T - \frac{q}{4\pi\lambda} \frac{a^2}{4\kappa_m t} (2 - \kappa_m/\kappa_w) \quad (7)$$

The second correction arises from the cylinder walls limiting heat exchange with the rest of the medium at a later stage in the measurement as the heat propagating radially from the wire begins to encounter the cylinder walls.

$$\delta T_2 = -\frac{q}{4\pi\lambda} \left\{ \ln \left(\frac{4\kappa t}{b^2 e^\gamma} \right) + \sum_{v=1}^{\infty} e^{-(g_v)^2 \kappa t / b^2} [\pi Y_0(g_v)]^2 \right\} \quad (8)$$

The terms in the second part of Eq. (8) (in series solution) are Bessel functions, where g_v are roots of Bessel functions $J_0(g_v)=0$ and Y_0 are Bessel functions of the second kind Table 1 gives first 5 terms applicable to series in Eq. (7).

Table 1 First 5 roots of Bessel functions $J_0(g_v)=0$ and Bessel functions $Y_0(g_v)$

v	g_v	$Y_0(g_v)$
1	2.4048	0.50993
2	5.5201	-0.33894
3	8.6537	0.27101
4	11.7315	-0.23243
5	14.9309	0.20643

It is important to note that in both correction terms (7) and (8), we require estimates of the parameters of the medium such as the product of density and specific heat capacity (ρc_p), and thermal diffusivity (κ). The error in the final computation of thermal conductivity depends (partly) on errors in the estimates of these unknown terms and is discussed in ‘Errors’.

THP – calculation method

To illustrate the calculation method, we work through the data set in Fig. 4. An initial λ estimate is calculated from a slope (λ_{exp}) using a linear least squares fit with

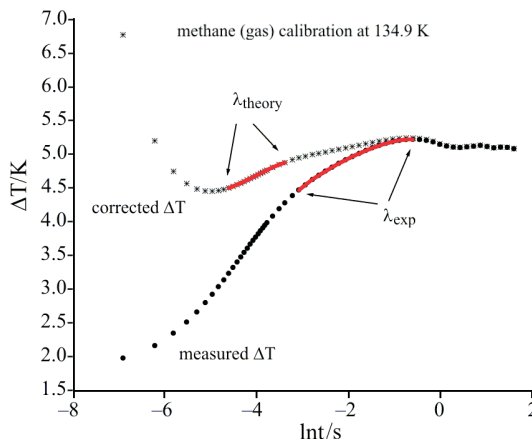


Fig. 4 The effect of applying corrections (7) and (8) to the raw (or measured) ΔT data. The corrected ΔT plot (and thus λ_{theory}) changes with each trial calculation of λ_{exp} using different numbers of ΔT , $\ln t$ points. Note the linear region for the calculation of λ also shifts after correction (on the ‘corrected ΔT ’ plot), away from the convection

correlation coefficient $R^2 \geq 0.90$ covering as many data points up to the maximum value just before convection starts (near the RHS of ΔT vs. $\ln t$ plot in Fig. 3).

$$\lambda_{\text{expt}} = \frac{I^2 R_0}{4\pi l [d(\Delta T)/d\ln t]} \quad (9)$$

where no corrections are applied to λ_{expt} .

The order in which corrections are applied is as follows: correction terms (7) and (8) are added to ΔT ,

followed by term (6), which is applied before taking the corrected value of thermal conductivity (λ_{theory}) – Fig. 4.

$$\Delta T_{\text{theory}} = \Delta T + \delta T_1 + \delta T_2 \quad \text{and}$$

$$\lambda_{\text{theory}} = \frac{1}{4\pi l [d(\Delta T_{\text{theory}})/d\ln t]} \cdot [I^2 R_0 + 2I^2 dR \ln t + I^2 dR \ln(4\kappa/a^2 e^\gamma)] \quad (10)$$

To complete the two correction terms in ‘Other corrections’, we need reference gas parameters. For the purpose of this calculation, we use values for nitrogen at 100 K and 1 atmosphere ($\lambda = 1.0845 \cdot 10^{-2} \text{ W m}^{-1} \text{ K}^{-1}$, $\rho = 3.4367 \text{ kg m}^{-3}$, $c_p = 1.0715 \cdot 10^3 \text{ J kg}^{-1} \text{ K}^{-1}$). These values are obtained from the NIST database [7], considered to be a *de facto* standard for pure gases in the measurable temperature and pressure range.

These reference values are deliberately chosen to be away from the actual values of methane at 134.9 K to illustrate the relative insensitivity of the final calculation to the reference parameters. Reference diffusivity $\kappa = \lambda/\rho c_p$ is 42% greater and ρc_p is 50% less than corresponding methane values.

If the estimate of λ_{expt} is below the true value, then the corrected value λ_{theory} , will be high and vice versa. The point at which the two λ values converge is taken to be the true value of the thermal conductivity. The exact region (and number of points) required for the calculation of each of the two slopes (λ_{expt} and λ_{theory}) are found by minimising the difference between λ_{expt} and λ_{theory} as shown in Fig. 5.

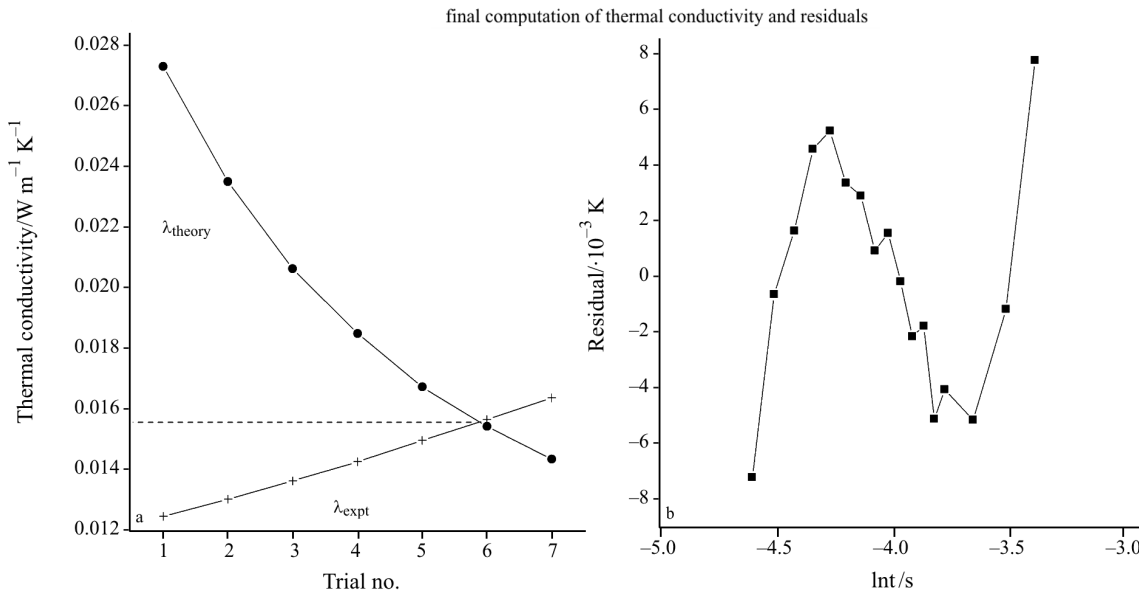


Fig. 5 a – The point at which λ_{expt} and λ_{theory} cross is taken as the value of thermal conductivity, but all pairs of λ_{expt} and λ_{theory} cover the true value. In the above case, each successive trial contains one less data point in the calculation of slope for λ_{expt} on the lower end of time axis (i.e. left hand side) – all other points for the calculation of the two slopes remain fixed. This convergence can be different from the actual value by over 2% if estimates of reference gas parameters are incorrect by 100%. b – Residuals are approximately an order of magnitude less after applying corrections (c.f. Fig. 3 residuals). Still some small error(s) remain as can be seen from this residual plot. Error on ΔT_{theory} is reduced to $\pm 0.09\%$

Table 2 Thermal conductivity measurements over Titan's temperature range show this sensor is able to measure with good accuracy under laboratory calibration conditions

Temperature/K	Medium	Measured $\lambda/W\ m^{-1}\ K^{-1}$	Reference $\lambda/W\ m^{-1}\ K^{-1}$	Error/%	Final λ_{exp} interval (Int)
94	N ₂	0.0102	0.0102	0	-2.501 to -1.033
100	N ₂	0.0107	0.0108	-0.9	-2.501 to -1.474
120	CH ₄	0.0136	0.0135	+0.7	-3.219 to -0.738
143	CH ₄	0.0163	0.0162	+0.6	-3.219 to -1.033
172	CH ₄	0.0193	0.0195	-1.0	-3.772 to -0.592
187	CH ₄	0.0211	0.0213	-0.9	-3.65 to -0.592
203	C ₂ H ₆	0.0123	0.0123	0	-3.219 to -0.622

The λ value measured by this method is $0.0154\ W\ m^{-1}\ K^{-1}$; on comparison with the standard value from [7] of $0.0153\ W\ m^{-1}\ K^{-1}$, we can see that the error is small (<1%) despite an approximately 50% deviation in reference gas parameters. The advantage of this processing technique is that the closest pair of λ_{exp} and λ_{theory} confine the absolute error in measurement and does not require exact knowledge of the medium being measured.

Table 2 gives more examples of measurements made by this sensor during calibration.

Errors

Thermal conductivity calculations using the above technique can yield very accurate values with the principal source of error resulting from large discrepancies in the estimates of reference parameters ρc_p and κ . Nitrogen serves as good reference for interpreting calibration data for short chain hydrocarbons (methane and ethane).

Empirical evidence (from several calculations of λ of pure methane and ethane at various temperatures) suggests that if nitrogen is chosen as reference at the correct temperature and pressure, then the errors in ρc_p and κ are limited to $\pm 30\%$ (according to outputs from [7]) and therefore the error on λ can be confined to 0.5% for laboratory measurements (where vertical temperature gradients in the measurement cell are kept to a minimum).

Errors need to be minimised at the time of designing the instrument. In general, precautions need to be taken for contacts to be good (i.e. no contact or other parasitic resistance should be present). Also the line source (central wire) should be of high purity platinum with no kinks or deformities along the wire. It is very important to keep the heat flux constant by designing a constant power source. Coarse sampling time steps, where λ values either undershoot or overshoot the actual value can also introduce errors, but

this can be taken care of by experimental design. Ideally the instrument should consist of two cells of different lengths with both exposed to the medium being measured so edge effects can be subtracted.

For low pressure applications, where the mean free path of the gas is comparable to the wire radius, the wire must be as thin as possible for the line source approximation to hold. Resistance as a function of temperature calibration for the whole thermal conductivity instrument is vital.

Conclusions

The thermal conductivity calculations performed on calibration data over the low temperature range from 80 to 170 K show the results are extremely accurate and fall within a 1% error band of the actual or published values.

The actual (or reference) thermal conductivity values are obtained from NIST [7] and we do not consider errors within NIST as this combination of database and software is an acceptable bench mark in thermophysical measurements for pure gases. There might be significant errors (<10%) in NIST near the boiling point region (i.e. change of state/condensation).

Acknowledgements

The thermal conductivity instrument (THP) is a part of the surface science package (SSP) on board the Huygens probe. The SSP project has been predominantly funded by the Particle Physics and Astronomy Research Council (PPARC), with support from the Polish Academy of Sciences.

References

- 1 P. N. W. Birchley, *et al.*, Proc. Symposium on Titan, ESA SP-338 (1992) 311.
- 2 J. C. Zarnecki, *et al.*, ESA SP-1177 (1997) 177.
- 3 J. C. Zarnecki, *et al.*, Space Sci. Rev., 104 (2002) 593.

- 4 J. J. de Groot, *et al.*, *Physica*, 75 (1974) 454.
- 5 J. J. Healy, *et al.*, *Physica*, 82C (1976) 392.
- 6 H. S. Carslaw and J. C. Jaeger, *Conduction of Heat in Solids*, 2nd Ed., Oxford University Press, London 1959.
- 7 National Institute of Standards and Technology, *Standard Reference Database*, 14 (NIST14) Version 9.09 (1993).
- 8 J. C. Jaeger, *Austr. J. Phys.*, 36 (1955) 167.
- 9 M. Banaszkiewicz, *et al.*, *Rev. Sci. Instrum.*, 68 (1997) 4184.
- 10 W. A. Wakeham, *et al.*, *Experimental Thermodynamics III, Measurement of Transport Properties of Fluids – Chemical Data Series*, No. 37, Blackwell Scientific Publications, Oxford 1991.

Received: March 23, 2006

Accepted: April 26, 2006

DOI: 10.1007/s10973-006-7607-1